

NUCLEAR DATA AND MEASUREMENTS SERIES

**ANL/NDM-8
Fast Neutron Capture and Activation Cross Sections
of Niobium Isotopes**

by

W.P. Poenitz

June 1974

**ARGONNE NATIONAL LABORATORY,
ARGONNE, ILLINOIS 60439, U.S.A.**

NUCLEAR DATA AND MEASUREMENTS SERIES

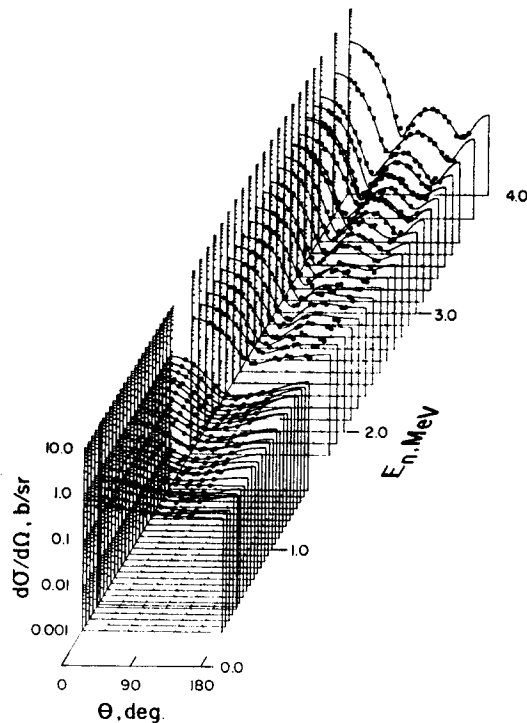
ANL/NDM-8

FAST NEUTRON CAPTURE AND ACTIVATION
CROSS SECTIONS OF NIOBIUM ISOTOPES

BY

W. P. Poenitz

May 1974



ARGONNE NATIONAL LABORATORY,
ARGONNE, ILLINOIS 60439, U.S.A.

The facilities of Argonne National Laboratory are owned by the United States Government. Under the terms of a contract (W-31-109-Eng-38) between the U. S. Atomic Energy Commission, Argonne Universities Association and The University of Chicago, the University employs the staff and operates the Laboratory in accordance with policies and programs formulated, approved and reviewed by the Association.

MEMBERS OF ARGONNE UNIVERSITIES ASSOCIATION

The University of Arizona
Carnegie-Mellon University
Case Western Reserve University
The University of Chicago
University of Cincinnati
Illinois Institute of Technology
University of Illinois
Indiana University
Iowa State University
The University of Iowa

Kansas State University
The University of Kansas
Loyola University
Marquette University
Michigan State University
The University of Michigan
University of Minnesota
University of Missouri
Northwestern University
University of Notre Dame

The Ohio State University
Ohio University
The Pennsylvania State University
Purdue University
Saint Louis University
Southern Illinois University
The University of Texas at Austin
Washington University
Wayne State University
The University of Wisconsin

NOTICE

This report was prepared as an account of work sponsored by the United States Government. Neither the United States nor the United States Atomic Energy Commission, nor any of their employees, nor any of their contractors, subcontractors, or their employees, makes any warranty, express or implied, or assumes any legal liability or responsibility for the accuracy, completeness or usefulness of any information, apparatus, product or process disclosed, or represents that its use would not infringe privately-owned rights.

ANL/NDM-8
FAST NEUTRON CAPTURE AND ACTIVATION
CROSS SECTIONS OF NIOBIUM ISOTOPES

BY
W. P. Poenitz
May 1974

Applied Physics Division
Argonne National Laboratory
9700 South Cass Avenue
Argonne, Illinois 60439
U.S.A.

TABLE OF CONTENTS

	<u>Page</u>
ABSTRACT.	3
I. INTRODUCTION.	4
II. MEASUREMENTS OF THE $^{93}\text{Nb}(n,\gamma)^{94}\text{Nb}$ CROSS SECTION	5
1. Experimental Set-Up and Procedure	5
2. Measurements and Normalization.	6
3. Corrections	7
4. Experimental Results and Uncertainties.	9
5. Comparison with Other Data.	10
III. NEUTRON CAPTURE AND GAMMA CASCADE STATISTICAL MODELS.	10
1. Neutron Capture and Activation Cross Sections.	10
2. Level Density	12
3. Neutron and Gamma Transmission Coefficients	14
4. Low Level Occupation Probability.	14
IV. MODEL CALCULATIONS AND RESULTS.	15

FAST NEUTRON CAPTURE AND ACTIVATION
CROSS SECTIONS OF NIOBIUM ISOTOPES

BY

W. P. Poenitz

ABSTRACT

The radiative neutron capture cross section of ^{93}Nb was measured from 0.3 MeV to 2.5 MeV. A large liquid scintillator and the time-of-flight technique were used to detect the prompt capture γ -rays. A grey neutron detector was employed as a neutron flux monitor. The data were normalized at 0.5 MeV to the capture cross section of ^{197}Au .

Capture and activation cross sections of ^{93}Nb and ^{94}Nb were calculated in terms of the statistical model of Hauser and Feshbach and the statistical gamma cascade model reported previously.

*This work was performed under the auspices of the U.S. Atomic Energy Commission.

I. INTRODUCTION

Fast neutron capture cross sections are of importance in fission and fusion reactor design. There is additional interest from the standpoint of astrophysical concepts of the creation of the elements, and nuclear reaction theory. The capture cross sections of many isotopes are difficult to measure if these isotopes are unstable and decay with a short half life. This is the case for many fission product nuclei which are of importance in reactor neutronics. Thus, the calculation of capture cross sections with a theoretical model and the testing of such model calculations with cross sections of stable isotopes for which reasonable data are available is of interest. Unfortunately, some such model calculations fail to reproduce measured data by a factor of two (1) or results from different model calculations may be discrepant up to an order of magnitude (2).

Neutron capture cross sections in the keV-MeV range are a small fraction of the total cross sections and with some exceptions, difficult to measure. A capture event may be detected by one of the effects it causes:

- a. the production of an isotope with the mass $A+1$.
- b. the capture γ -rays emitted during the de-excitation of the compound nucleus.
- c. the radioactive product nuclei, or
- d. the loss of a neutron from the incident beam.

Technique a, is usually applicable only at thermal neutron energies where the capture cross sections of some nuclei are very large. Technique c, is the most precise technique, though only applicable in cases where the capture process results in a radioactive residual nucleus with a well-known decay scheme. Technique d, may be used only if the capture cross section is identical with the absorption cross section. Thus, the detection of the capture γ -rays is the only universal technique for the measurement of neutron capture cross sections. Several methods have been developed for the detection

of prompt capture γ -rays. The two principle ones utilize a large liquid scintillator (3) or the Moxon-Rae detector (4).

Niobium is of special interest as a first wall and structural material in possible fusion reactors. Capture and activation cross sections of ^{93}Nb and ^{94}Nb are needed for the consideration of breeding ratios and after-heat problems. The present report describes measurements of the capture cross section of ^{93}Nb and model calculations of the capture and activation cross sections of ^{93}Nb and ^{94}Nb in the energy range from 0.3 MeV to 2.5 MeV. A large liquid scintillator was used. This detector allows discrimination against other γ -producing events such as the $(n, n'\gamma)$, and the $(n, \gamma n')$ reactions.

II. MEASUREMENTS OF THE $^{93}\text{Nb}(n, \gamma)^{94}\text{Nb}$ CROSS SECTION

1. Experimental Set-Up and Procedure

The experimental set-up is schematically shown in Fig. 1. A pulsed and bunched proton beam was accelerated by the Argonne tandem-dynamitron. The repetition rate was 2 Mhz and the pulse-width was 1 - 2 nsec. Metallic lithium targets with thicknesses between 40 and 100 μm were used for the production of neutrons in the energy range from 0.3 to 2.5 MeV. The lithium was evaporated on 0.025-cm thick tantalum backings. The neutron energy was determined from the known kinematic relations, the primary proton energies, the stopping cross sections and the target thicknesses. A 4π -neutron shield surrounding the source was used in order to reduce the γ -ray and neutron background of the detectors. A conical opening in the shield provided a collimated neutron beam. This beam was incident on the sample positioned in the center of the capture γ -ray detector. The neutron beam was finally captured in the neutron monitor which also acted as a neutron beam-catcher.

The capture γ -ray detector was a 1300-liter tank filled with a liquid scintillator formulated in this laboratory. The shape of the tank approximated a sphere in order to obtain the best signal-to-background ratio. The tank was made of iron and had a central channel

with a diameter of 10 cm. The inside surface of the tank was painted with an epoxy-based TiO-reflector. The scintillator was a mixture of psuedo-cumene, p-therphenyl, POPOP and boron-methyl. A continuous nitrogen gas flow was maintained through the scintillator at a low flow-rate in order to prevent poisoning of the scintillator by oxydation. The scintillation light was viewed by twelve AVP57 multipliers which were distributed equally over the surface of the tank. A rise-time correction was applied using the on-line computer. The time-resolution of the tank was 3 - 4 nsec and the γ -energy resolution was 26 percent for ^{60}Co , and 53 percent for ^{137}Cs (FWHM). The tank was shielded by 10-20 cm of lead, 60 cm of concrete, and, partially, by 2-4 cm of low-background iron. The flight path from source to sample was 250 cm. This was sufficient to separate, by time-of-flight, the low-energy neutron group of the $^7\text{Li}(p,n)$ source reaction over the entire energy range of the present measurements.

The samples used in the present experiment consisted of metallic discs with a diameter of 8.9 cm and a thickness of about 0.07 cm. Between 2 and 4 niobium discs were stacked to form one sample. Only one gold sample disc was used for normalization measurements. A computer controlled automatic sample transport system provided for the exchange of the niobium and gold samples in the ratio measurements.

The Grey Neutron Detector (5) was used as a neutron monitor. This detector has been described on several occasions (6-8). Because the cross section of niobium was normalized at 500 keV with a measurement relative to the standard capture cross section of gold, only the shape of the neutron detector efficiency was needed for the present measurements. The use of this detector even up to 2.5 MeV appears appropriate considering the larger uncertainties caused by other quantities.

2. Measurements and Normalization

An on-line computer system (9) was used for the data acquisition and analysis. The time-of-flight spectrum of the capture γ -ray detector, the energy spectra coincident with the neutron peak in the time-of-flight spectrum, and the energy spectra coincided with an adjacent

equal-size background time interval were recorded. The threshold for the energy pulse-height was usually set in the 2.5 - 3.0 MeV region in order to eliminate the detection of $(n, n'\gamma)$ and $(n, \gamma n')$ processes. However, for the measurement relative to gold at 0.5 MeV the threshold was set as low as 0.8 MeV. Fig. 2 shows typical energy spectra obtained for niobium at 0.5 and 2.0 MeV incident neutron energies with this capture γ -ray detector. The background was subtracted by using the spectra collected for the time range adjacent to the neutron peak. The number of capture events was obtained by integrating over the neutron peak in the time-of-flight spectrum and subsequently correcting for the detection efficiency. The latter was obtained by utilizing the measured γ -energy spectra.

The spectrum obtained from the neutron monitor was recorded simultaneously with the on-line computer. Dead-time corrections were essentially eliminated in this procedure because the computer input and storage-cycle causes the major dead-time.

The background of the γ -ray detector was suppressed by the time-of-flight technique. Checks for additional background from neutrons scattered in the sample were carried out by using scattering samples with a negligible capture cross section (lead). The background of the neutron monitor was determined with a plugged collimator. This latter background was quite small for the present well-shielded set-up.

3. Corrections

The major correction in the present experiment is that for capture events caused by neutrons which were scattered once or several times within the sample. The reason for large corrections at high neutron energies is the small size of the capture cross section compared to the elastic and inelastic scattering cross sections. Inelastic scattering events transfer neutrons into an energy range where the capture cross section is up to one order of magnitude larger than for the primary neutrons. At 2.5 MeV incident neutron energy capture events caused by scattered neutrons contribute 50 to 150 percent to the primary capture rate, depending on the thicknesses of the niobium samples.

The correction for the capture of scattered neutrons was calculated with the Monte Carlo technique. The energy loss in the inelastic scattering process, the angular distribution in a primary elastic scattering process, and the energy dependence of the three cross sections (elastic, inelastic and capture) were taken into account. Input data were primarily selected from a recent cross section evaluation of niobium by Smith et al. (10). A neutron was followed up to three collisions in the sample. Capture events from subsequent collisions were assumed to be reduced by the same factor as capture events at the third collision were reduced compared with capture events at the second collision. The latter assumption caused only a 1 percent change of the total correction. The correction which includes the neutron flux attenuation in the sample is shown for different sample thicknesses in Fig. 3. In order to check the validity of the scattering correction, measurements were carried out for different sample thicknesses at 0.5 and 2.5 MeV incident neutron energy. The corrected specific capture rates agreed to well within the statistical uncertainties.

The limitation for the precision of capture cross section measurements with the present technique is largely determined by the uncertainty of the extrapolation of the measured capture γ -ray pulse height spectra to zero pulse height (11). The spectra shown in Fig. 4 were obtained for the lowest threshold used in the present experiment (0.8 MeV). The background of the large liquid scintillator increases rapidly with decreasing pulse height. Thus, for small pulse-heights, the spectra in Fig. 4 were obtained as a small difference of large numbers. The resulting uncertainty in this low energy range causes the uncertainty of the extrapolation to zero pulse-height. The extrapolation which was used is shown in the figures.

The efficiency for the detection of capture events is determined by the threshold-setting for the discrimination against background, the leakage of γ -rays out of the scintillator tank, and the absorption of γ -rays in the sample and channel-wall material. The latter two effects are in the 1-3 percent range and were calculated with the

Monte Carlo technique. The major correction for the shape of the tank-efficiency comes from the change of the total γ -cascade energy caused by the change of the primary neutron energy. A correction was calculated using the average between two assumed shapes for the γ -ray pulse-height spectra (rectangular and triangular).

Additional corrections were made for the neutron flux attenuation in the samples and in the air between the sample and the neutron detector. The deviation of the neutron detector efficiency from an energy independent constant (straight line) was corrected for as previously described (7,8). Corrections for non-monoenergetic neutrons from the neutron source were applied as described on another occasion (12).

4. Experimental Results and Uncertainties

The values obtained for the shape of the niobium capture cross section were normalized with the measurements relative to the standard capture cross section of gold at 0.5 MeV. The value obtained for this ratio was

$$\frac{\sigma_{n,\gamma}({}^{93}\text{Nb}, 0.5 \text{ MeV})}{\sigma_{n,\gamma}({}^{197}\text{Au}, 0.5 \text{ MeV})} = 0.376 \pm 0.017$$

A value of 138 mb was used for $\sigma_{n,\gamma}({}^{197}\text{Au}, 0.5 \text{ MeV})$. This value was obtained in an evaluation of a consistent set of data for $\sigma_{n,\gamma}({}^{197}\text{Au})$, $\sigma_{n,\gamma}({}^{238}\text{U})$, $\sigma_{n,f}({}^{235}\text{U})$, and $\sigma_{n,\alpha}({}^6\text{Li})$ (13). Thus the result for niobium is

$$\sigma_{n,\gamma}({}^{93}\text{Nb}, 0.5 \text{ MeV}) = (51.9 \pm 3.5) \text{ mb.}$$

An uncertainty of 5 percent was assumed for the gold cross section. The results for the capture cross section of ${}^{93}\text{Nb}$ in the energy range from 0.3 MeV to 2.5 MeV, given in Table 1, were normalized with this value. E_n is the average neutron energy, and ΔE_n is the energy resolution. The energy uncertainty was estimated to be 3-4 keV, and thus unimportant for the present measurements. $\Delta\sigma_{n,\gamma}$ is the uncertainty of the measured capture cross section and was derived from the different contributions listed in Table 2. The uncertainties for some corrections are zero at the normalization point

(0.5 MeV) because these uncertainties were already included in the ratio measurement.

5. Comparison with Other Data

The experimental results are shown in Fig. 5. Also shown in this figure are the data reported by other experimentors in the energy range of the present measurements. The data by Stavisskii and Tolstikov (14) were obtained by detecting the 6.6 min activity of the isomeric state in ^{94}Nb . The thermal cross sections were used to eliminate the detection efficiencies. Thus, the experimental results for the fast energy range are only valid if the isomeric cross section ratio is energy independent. This assumption does not apply because the distribution of compound spins changes with energy. The values by Stavisskii and Tolstikov which are shown in the figure were corrected for this wrong assumption.

The data by Diven et al. (15) and by Stavisskii and Shapar (16) were also measured with a large liquid scintillator. All three data sets were measured relative to the fission cross section of U-235, though the indium activation cross section was used as an intermediate reference in the Russian measurements.

Though the error bars of most measurements still overlap there is a consistent difference by about 10-15 percent between the present data and those measured relative to U-235 fission. A similar difference can be found at energies below 150 keV where measurements by Gibbons et al. (17) and by Kompe (18) resulted in 10-30 percent lower values than those obtained relative to U-235 fission. Part of the discrepancies resolves when newer ^{235}U fission cross sections values are used as reference data.

III. NEUTRON CAPTURE AND GAMMA CASCADE STATISTICAL MODELS

1. Neutron Capture and Activation Cross Sections

Different mechanisms are in use to explain the neutron capture reaction in the keV-MeV energy range. In the energy range of the present measurements the major contribution comes from the formation of compound nuclei and their successive decay by γ -radiation. The

statistical theory by Hauser and Feshbach (19) was applied by Margolis (20) and Lane and Lynn (21) to derive the neutron capture cross section:

$$\sigma_{n,\gamma}(E) = \frac{1}{2(2I+1)} \frac{\pi}{k^2} \sum_{j=|\ell-j|}^{\ell+1/2} T_n(\ell j, E) \times$$

$$\times \sum_{j=|j-I|}^{j+I} \frac{(2J+1) T_\gamma(J, E) R}{T_\gamma(J, E) + \sum T_n(\ell' j', E, E_m)}$$

where the T_n are the neutron transmission coefficients, I is the spin of the target nucleus, k is the wave number, the J 's are the spins of the compound nucleus, ℓ the spin orbit momentums, j the channel spins, and E the energy. The sum in the denominator is over all neutron exit channels to the target nucleus levels labeled with m .

T_γ is $2\pi \langle \Gamma_\gamma \rangle / \langle D \rangle$, where $\langle \Gamma_\gamma \rangle$ is the average gamma width, and $\langle D \rangle$ the average level spacing. R is a correction for replacing the average over the ratios in above formula by the ratio of the averages of the individual quantities. For the present energy range this correction is of minor importance due to the large number of open channels.

Moldauer (22) pointed out the importance of the competition between neutron emission and γ -radiation in states above the neutron binding energy. Such states may be occupied after an initial γ -ray emission. This effect which results in $(n, \gamma n')$ reactions may be approximated for the present calculations by assuming that all levels, above the neutron binding energy, decay by neutron emission. Thus in the denominator of the above expression for the capture cross section

$$\Gamma_\gamma \sim \sum_{J'} \int_0^E W(E - E'; J, J') \rho(E' J') dE',$$

and in the numerator

$$\Gamma_c \sim \sum_{J'} \int_0^{B_n} W(E - E'; J, J') \rho(E' J') dE'$$

is used. Here $W(E - E')$ is the probability for a transition from the

compound state (energy E) to a lower lying level with the energy E'. ρ is the level density, and B_n the binding energy.

The decay of the compound nucleus by the emission of a γ -ray is usually only the first step in a γ -cascade. These cascades finally determine the occupation probability of the isomeric state (if existing) and the ground state, and thus their respective activation cross sections. Because of the large number of levels in medium and heavy weight nuclei even at lower excitation energy, the behavior of these cascades can be calculated with statistical assumptions. A model for this purpose has been described previously (23).

The level scheme is assumed to consist of a range in which the known level density formula applies and a lower region in which individual levels are known. The γ -cascades are followed in this E, J, π - space until the low lying levels are occupied. Using measured transition probabilities the final occupation probability for the ground state and the isomeric state can be obtained. Applications and tests of this model were reported by several authors (see for example Refs. 24-27).

For the calculation of the activation cross section, the probability for the occupation of the level of interest must be included in above formula; thus

$$\sigma_{act,i} = \frac{1}{2(2I+1)} \frac{\pi}{k^2} \sum_{j=|\ell-\frac{1}{2}|}^{\ell+\frac{1}{2}} T_n(\ell j, E) \times$$

$$\times \frac{\sum_{J=|j-I|}^{j+I} (2J+1) T_c(J, E) B_1(J, E)}{T_\gamma(J, E) + \sum T_n(\ell' j', E, E_m)} R = 1$$

The probability $B_1(J, E)$ depends on the compound spin J, the total cascade energy E, the level density, the transition probabilities and the energy, spin and parity of the level i, as previously described (23).

2. Level Density

The level density must be known in several stages of the calculations. The summation over the neutron transmission coefficients in the

denominator in the above formula requires the supplementing of known levels with such obtained from a level density formula. The calculation of the average γ -width requires a level density formula as indicated above, and finally, the γ -ray cascade statistics needs a level density formula.

The Fermi-gas model level density formula, modified for shell and pairing energy was used:

$$\rho(E, J) = \frac{2J+1}{2\sqrt{2\pi} \cdot \sigma^3} \exp\left(-\frac{(2J+1)^2}{8\sigma^2}\right) \rho(E)$$

$$\rho(E) = \frac{\sqrt{\pi}}{12 a^{1/4} E^{5/4}} \exp(2\sqrt{aE^*})$$

E^* is the effective excitation energy

$$E^* = E - \Delta,$$

where Δ is the pairing energy which reduces the excitation energy of even-even and even-odd nuclei. Nuclear shell effects were accounted for with

$$a = a_0 A^{3/2} (\bar{j}_z + \bar{j}_n + 1),$$

where A is the nuclear mass and a_0 is a constant. The \bar{j} are the average values of the total angular momentum for protons (z) or neutrons (n) over the shells near the Fermi-level. The spin cut-off factor σ depends on the nuclear temperature T and the momentum of inertia θ of the nucleus

$$\sigma^2 = \frac{T \cdot \theta}{2} = \sigma_0 \sqrt{a E} A^{2/3},$$

where σ_0 is a constant. Parameters from References 28-30 were used. The level density formula describes very well the level density at high energies, however, generally under evaluates the number of levels at low excitation energies. Thus a "back-shifted" Fermi-gas

model has been proposed in which Δ is used as a free adjustable parameter (31).

3. Neutron and Gamma Transmission Coefficients

The neutron transmission coefficients were calculated with the optical model code ABACUS (32). The spherical potential consisted of a Woods-Saxon real term, a derivative surface-imaginary term and a Thomas spin-orbit term. This type of potential was successfully used by Lambropoulos for an analysis of neutron interactions with the isotopes of molybdenum. The parameters

$$V_{\text{real}} = 50 \text{ MeV} \qquad W_{\text{imag}} = 6 \text{ MeV} \qquad V_{\text{s-o}} = 7 \text{ MeV}$$

$$R_{\text{real}} = 5.5 \text{ F} \qquad R_{\text{imag}} = 5.8 \text{ F}$$

$$A_{\text{real width}} = 0.69 \text{ F} \qquad A_{\text{imag width}} = 0.55 \text{ F}$$

and the energy dependence

$$V(E) = V - 0.25 E, \quad W(E) = W - 0.2 E, \quad E \text{ in MeV}$$

which were obtained by Smith et al. (10) from a fit of experimental scattering data, were used in the present calculations.

Gamma transmission coefficients were calculated with the formula given in Section 3.1. The Weisskopf estimates were used for the gamma transition probabilities (33). Dipole and quadrupole transitions were included. Average γ -widths calculated with these assumptions are known to be too large by one or two orders of magnitude. Thus only the energy dependence was used and the values were normalized with experimental data from the eV-energy range.

4. Low Level Occupation Probability

Fig. 6 shows the level scheme of ^{94}Nb used in the present calculations. The γ -cascades deexciting compound states with the spins 4 and 5 are shown in schematic. The transition probabilities for the decay of the low lying states, their energies, and spins were obtained from thermal neutron capture gamma-ray spectroscopy

measurements (34). The calculations of the $B(J,E)$ were carried out with the code CASCADE (23). Several γ -transition ratios measured in eV-resonances are available for checking the cascade model for niobium. Thomas (35) measured the ratio of the 99 keV transition (from the 140 keV, 2^- level to the 41 keV, 3^+ level) to the 113 keV transition (from the 113 keV, 5^+ level to the ground state) and obtained 1.64 for the spin 4 resonances and 0.88 for the spin 5 resonances. The calculations with CASCADE yield 1.56 and 0.80 for the two different spins which is in very good agreement with the experimental values. For the ratio of the 293 keV transition (from the 334 keV, 2^+ level to the 41 keV, 3^+ level) to the 113 keV transition Thomas obtained 0.65 and 0.24 for the 4^+ and 5^+ resonances which again confirms the theoretical model which yields 0.56 and 0.23.

Using the low level occupation probability for the isomeric state and the thermal capture cross section, the thermal activation cross section can be calculated. A value of 0.63 barns is obtained for a spin 5 and 0.81 barns for a spin 4. This gives the range in which the actual cross section should be. The experimental value is unfortunately very uncertain (1.0 ± 0.5 b) but overlays with this range.

IV. MODEL CALCULATIONS AND RESULTS

The calculations of capture and activation cross sections were carried out with the models described above. For ^{93}Nb the values for $\langle \Gamma_\gamma \rangle / \langle D \rangle$ were normalized with experimental values observed for resonances in the eV-energy range (36). Levels of ^{93}Nb which were missing at higher energies were corrected for with the help of the level density formula. The constant a_0 in the level density formula was increased by 10 percent in order to obtain the experimentally observed level density of ^{94}Nb at $E \sim B_n$.

$\langle \Gamma_\gamma \rangle / \langle D \rangle$ was increased for a better fitting of the experimental value. The values for $\langle \Gamma_\gamma \rangle$ were greatly changed between the second and the third edition of Ref. 36. The present cross sections are much better fitted with values for $\langle \Gamma_\gamma \rangle$ from the older edition.

The results from the model calculations for ^{93}Nb are shown in Fig. 7. The experimental values from the present measurements are also shown. There are no experimental values known for the activation cross sections in the present energy range. The cross sections shown are those for the prompt formation of the 6.3 min and $2 \cdot 10^4$ y activities. The isomeric state eventually decays with 99.9 percent into the ground state of ^{93}Nb , thus the final formation of the $2 \cdot 10^4$ y activity is described by the capture cross sections. The neutron capture cross section is strongly dependent on competitive decay probabilities of the compound nucleus. Thus, it is satisfactory that the total inelastic scattering cross section of ^{93}Nb is very well described with the parameters used in the present calculations. This is shown in Fig. 8 where the calculated total inelastic cross section is compared with the evaluated cross sections by Smith et al. (10). A 20 percent uncertainty was assumed for the latter.

Model parameter values are sparse for ^{95}Nb . No experimental values were known to check the level density formula for ^{95}Nb and only two values for $\langle \Gamma_{\gamma} \rangle$ are known (36). Low lying levels of ^{94}Nb and ^{95}Nb were obtained from the Nuclear Data Sheets (34). The results from the model calculations are shown in Fig. 9.

The fact that no experimental values of $\langle \Gamma_{\gamma} \rangle / \langle D \rangle$ exist introduces large uncertainties in the calculation of the cross sections for ^{94}Nb . The solid curves in Fig. 9 were calculated using two values of $\langle \Gamma_{\gamma} \rangle$ measured for otherwise unidentified resonances in ^{94}Nb , and the $\langle D \rangle$ obtained from the level density formula. The dashed curves were obtained by increasing $\langle \Gamma_{\gamma} \rangle / \langle D \rangle$ just as the values were increased for ^{93}Nb . The calculated values are uncertain by about a factor of 2 as indicated by the difference between the two sets of curves. The capture cross section for ^{94}Nb is smaller than that for ^{93}Nb (in the energy range of the present considerations). The reason can easily be understood by considering Fig. 10. ^{93}Nb and ^{95}Nb are odd-even nuclei, whereas ^{94}Nb is an odd-odd nucleus. The level density in ^{94}Nb is larger than in both, ^{93}Nb and ^{95}Nb . An energy gap due to the pairing energy exists in the latter two. Thus, the compound nucleus ^{94}Nb has a relatively low probability for

the re-emission of a neutron ((n,n) and (n,n') process) due to the low level density in ^{93}Nb , and a relatively high probability for a γ -emission due to the high level density of ^{94}Nb . On the other hand, the compound nucleus ^{95}Nb has a relatively large probability for the decay by neutron emission and a reduced probability for the emission of γ -rays.

REFERENCES

1. V. Benzi and M. V. Bartolani, IAEA-Conf. on Nucl. Data for Reactors, Vol. I, CN-23/115, Vienna (1967).
2. F. Schmittroth and R. E. Schenter, HEDL TME 73-63, UC-79, 79d, ENDF-194 (1973).
3. F. Reines, C. L. Cowan, Jr., F. B. Harrison, and D. S. Carter, Rev. Sci. Instr. 25, 1061 (1954).
4. M. C. Moxon and E. R. Rae, Nucl. Instr. and Methods 24, 445 (1963).
5. W. P. Poenitz, Nucl. Instr. and Methods 58, 39 (1968).
6. W. P. Poenitz and E. Wattecamps, EANDC-33 "U", 102 (1963).
7. W. P. Poenitz, Nucl. Instr. and Methods 72, 120 (1969).
8. W. P. Poenitz, Second IAEA Panel on Neutron Standard Reference Data, Vienna (1972).
9. W. P. Poenitz and J. F. Whalen, ANL-8026 (1973).
10. A. B. Smith, J. F. Whalen and P. T. Guenther, AP/CTR/TM-4 (1973).
11. R. C. Block and R. W. Hockenbury, EANDC-Symp. on Neutron Standards and Flux Normalization, p. 355, Argonne (1970).
12. W. P. Poenitz, Nucl. Sci. Engineering, 53, 370 (1974).
13. W. P. Poenitz, Symp. on Neutron Standards and Flux Normalization, p. 331 Argonne (1970).
14. Yu. Ya. Stavisskii and V. A. Tolstikov, Sov. J. Atomic Energy 9, 942 (1961).
15. B. C. Diven, J. Terrell and A. Hemmendinger, Phys. Rev. 120, 556 (1960).
16. Yu. Ya. Stavisskii and A. V. Shapar, Sov. J. Atomic Energy 10, 255 (1962).
17. J. H. Gibbons, R. L. Macklin, P. D. Miller and J. H. Neiler, Phys. Rev. 122, 182 (1961).
18. D. Kompe, Nucl. Phys. 133, 513 (1969).
19. W. Hauser and H. Feshbach, Phys. Rev. 87, 366 (1952).
20. B. Margolis, Phys. Rev. 88, 327 (1952).
21. A. M. Lane and J. E. Lynn, Proc. Phys. Soc. A70, 557 (1957).
22. P. A. Moldauer, Conf. on Neutron Cross Sections and Technology, Washington (1966).
23. W. P. Poenitz, Z. f. Physik 197, 262 (1966).

24. T. V. Egidy, Thesis, Techn. Hochschule Munich (1968).
25. A. Larshmana Rao, J. Rama Rao, Phys. Rev. Abstracts 3,14, 27 (1972).
26. W. P. Poenitz and J. R. Tatarczuk, Nucl. Phys. A151, 569 (1970).
27. A. Paulsen, Z. f. Physik 205, 234 (1967).
28. A. V. Malyshev, Soviet Physics JETP 18, 221 (1964).
29. P. E. Nemirovsky and Yu. V. Adamchuk, Nucl. Phys. 39, 551 (1962).
30. N. N. Abdelmalek and V. S. Stavinsky, Nucl. Phys. 58, 601 (1964).
31. H. Vonach, Technische Hochschule Munich, E14 1+2 (1973).
32. E. H. Auerbach, BNL-6562 (1962).
33. J. M. Blatt and V. F. Weisskopf, Theoretical Nuclear Physics, John Wiley & Sons, N. Y. (1952).
34. Nuclear Data Sheets for A=93, A=94, and A=95.
35. B. W. Thomas and T. J. Haste, Priv. Communication.
36. S. F. Mughabghab and D. I. Garber, Neutron Cross Sections, Vol. I, Resonance Parameters, Third Ed., BNL-325 (1973).

Table 1. Experimental Results for the ^{93}Nb Capture Cross Section

E_n /MeV	ΔE_n /MeV	$\sigma_{n,\gamma}$ /mb	$\pm \Delta\sigma_{n,\gamma}$ /mb
0.300	0.027	57.5	4.7
0.400	0.027	55.9	4.2
0.500	0.026	51.9	3.5
0.600	0.025	49.5	3.5
0.700	0.024	49.2	3.6
0.850	0.023	45.9	3.7
0.900	0.023	43.9	3.3
1.000	0.022	36.8	3.0
1.100	0.022	28.1	2.6
1.200	0.021	23.5	1.8
1.300	0.021	20.3	1.9
1.400	0.020	21.3	2.7
1.500	0.020	17.5	1.8
1.700	0.019	13.0	1.1
2.000	0.018	10.4	1.0
2.500	0.017	6.4	0.7

Table 2. Uncertainties of the Capture Cross Section Measurements

Source	Uncertainty Range/Percent
Statistics	1.5 - 10.4
Normalization	6.7
Neutron Monitor Efficiency	0.0 - 2.6
Capture Detector Efficiency	0.0 - 1.5
Correction for Scattered Neutrons	0.0 - 6.0
Correction for Scattering in Air	0.0 - 0.3

FIGURE CAPTIONS

- Fig. 1. Schematic of the Experimental Set-up.
- Fig. 2. Pulse-height Spectra obtained for Neutron Capture in Niobium at 0.5 and 2.5 MeV.
- Fig. 3. Correction for Capture of Neutrons Scattered in the Sample.
- Fig. 4. Pulse-height Spectra obtained for Neutron Capture in Niobium and in Gold at 0.5 MeV.
- Fig. 5. Comparison of Present Experimental Results with other Data. (Ref. 14-16).
- Fig. 6. Level Scheme and Gamma Cascades for ^{94}Nb .
- Fig. 7. Experimental Data for the Capture Cross Section of ^{93}Nb .
- Fig. 8. Model Calculation for the Total Inelastic Scattering Cross Section.
- Fig. 9. Model Calculations for the Capture and Activation Cross Sections of ^{94}Nb .
- Fig. 10. Schematic Comparison of Capture Probabilities in ^{94}Nb and ^{95}Nb .

